A MATHEMATICAL MODEL FOR SIMULATION OF LARGE SCALE ELECTROSTATIC PRECIPITATORS

B. Bellagamba, E. Lami, F. Mattachini
ENEL S.p.A., Centro Ricerca Termica e Nucleare
Via A. Pisano, 120
56122 Pisa, Italy

I. Gallimberti, R. Turri
Università di Padova, Dip. Ingegneria Elettrica
Via Gradenigo 6/a
35131 Padova, Italy

A. Gazzani, U. Tromboni
1999 Informatica Ricerca Sviluppo S.C.r.l.
Via C. Cassan, 34
35121 Padova, Italy

A. Pasinetti, R. Sala
MATEC s.r.l.
Via P. Rondoni, 11
20146 Milano, Italy

Abstract

Within the framework of the research program on thermal power plants flue gas treatment, ENEL (Italian Electricity Board) has started to develop a comprehensive mathematical model for simulating the operating conditions of large scale electrostatic precipitators.
The model, completely modular, will enable time-resolved simulations of the electrostatic precipitation phenomena, catering for all the relevant electric and transport processes which are known to occur.
Each specific process (e.g. corona discharge, particle charging, particle collection, rapping, reentrainment, etc.) is represented by a self-consistent mathematical model based entirely on the relevant physical laws.
Laboratory measurements on test cells under controlled conditions will be used both to obtain necessary basic information and for the separate validation of each module.

1. Introduction

The protection of environment has become, in the last years, a crucial problem of public concern, and the authorities are requested to set increasingly more stringent limits for the emissions of solid particulate as well as other gaseous pollutants from the industrial plants.

Electrostatic precipitators, that are the most widely used systems for solid particulate removal from combustion flue gases, have reached fairly good collection efficiencies. However it should be pointed out that this increase in efficiency has been obtained in general by increasing the collection area, with little, if any, improvement in the design. For example electrostatic precipitators still present a moderate efficiency in removing submicronic particles, the most dangerous for human health, or a progressive decrease in collection efficiency when fuel oil ash is concerned. This fact is particularly important in the Italian context, since a large percentage of Italian thermal power plants burn fuel oil.
The need of increasing the precipitators efficiency to cope with the new limits on emissions, together with a desire to fully understand the complex phenomena involved in the operation of such plants, have induced ENEL to promote a comprehensive research program on electrostatic precipitators. For a detailed study of the precipitation process a new numerical model was needed, a model capable to simulate from a physical point of view the different phenomena that take place in an electrostatic precipitator, and not based on semi-empirical approaches, such as the Deutsch approximation, or requiring the use of experimental data available from previous installations.
For the purpose of model validation a series of laboratory tests, which are described in a companion paper[1], has also been planned in order to collect a variety of information not easily obtainable from field measurements in industrial plants.
Such a new predictive model is considered of noteworthy importance to rationally evaluate the collection efficiency of the electrostatic precipitators installed in Italian thermal units, precipitators of different generations and therefore not comparable as regards design and dimensioning criteria. Moreover, it should be an useful tool for :

- a better evaluation of the performance obtainable by retrofitting existing plants;
- assessing of the values warranted by different builders;
- a wiser characterization of the remedies to apply to ill-working precipitators.

2. Model description

The numerical model of ESP operation is being developed with the aim of obtaining a useful tool to analyze the behaviour of electrostatic precipitators and to evaluate their performance under different operating conditions.
It will describe in time and space the mechanical, electrical, physical and chemical processes that are involved in transport, charging, migration and collection of fly ash.
Each of these major aspects constitutes a separate section of the model, within which more detailed phenomena can be represented.
The complete model is therefore structured into several modules, each one dealing with a particular process, solving a self-consistent set of integral-differential equations, and exchanging with the other modules the necessary information.

In this manner the model is "open", with the possibility of subsequently implementing, for instance, a more detailed description of some phenomena which, at present, are not considered of crucial importance for the general model. A schematic flow-chart, showing the interactions among modules, is represented in Figure 1. The model is organized into the follwing four sections :

- gas and particles motion
- electric field and discharge processes
- particle charging and migration
- particle collection

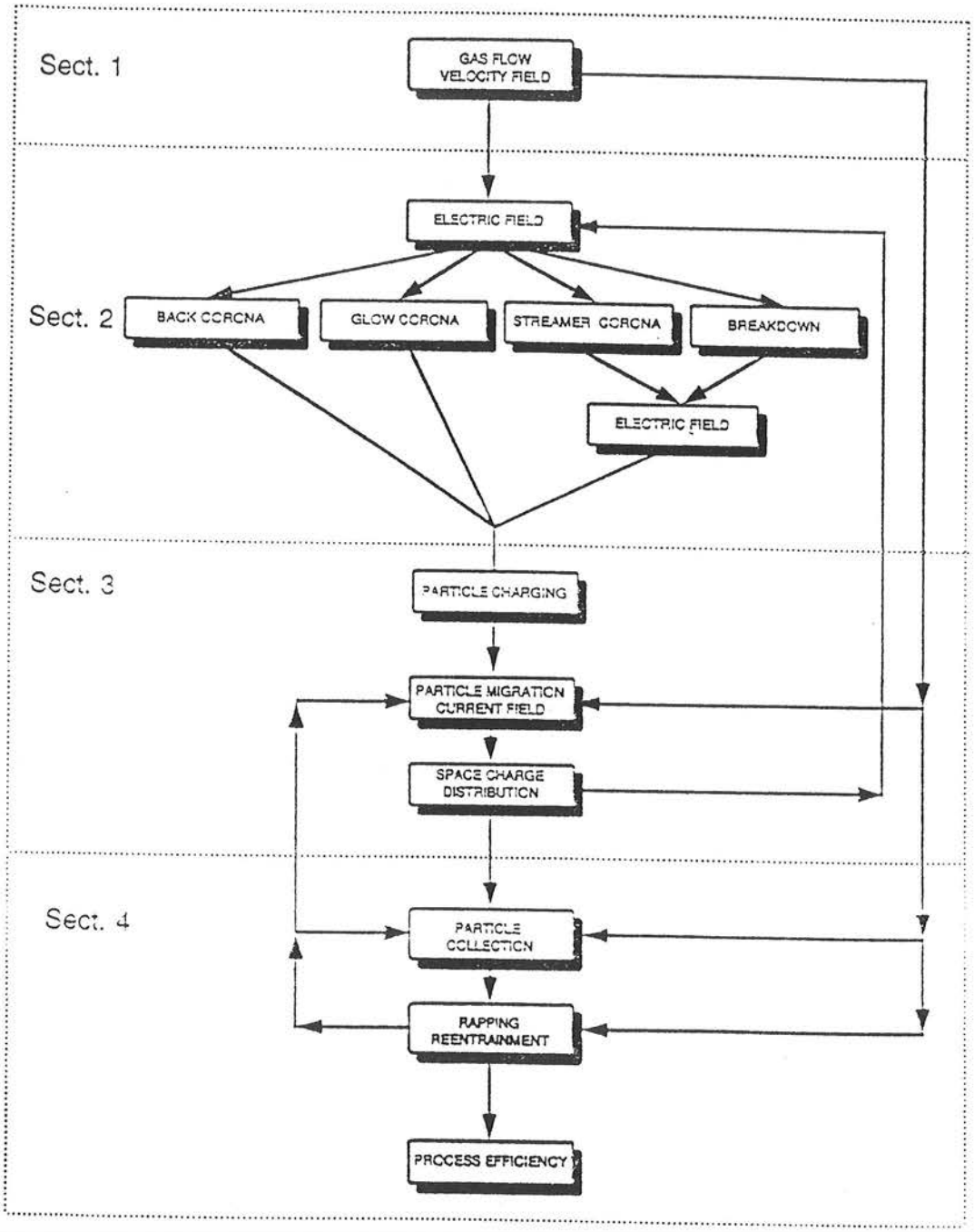

Fig.1 Schematic flow-chart of the ESP mathematical model.

The first section is constituted by the *Gas flow and velocity field* module. It evaluates the actual fluid-dynamic conditions of gas motion inside the ESP, and the velocity field of the gas that drags the dust particles. Almost all the modules of subsequent sections use the data calculated by this section. The underlaying hypothesis assumed in this module is a complete independence of the gas motion from the dispersed particles. Such hypothesis has been substantially confirmed by the first laboratory tests.

The second section contains the modules *Electric field, Back corona, Glow corona, Streamer corona* and *Breakdown*.
The module *Electric field* solves the Laplace or Poisson equations to determine the electric field distribution within the precipitator ducts. The corona modules simulate the ionic charge injection into the interelectrodic space during the time evolution of the system. *Glow corona* simulates the continuous inlet of positive and negative charges into the interelectrodic region in DC regimes, while *Streamer corona* simulates the (almost) instantaneous charge deposition all over the interelectrodic space due to an impulse streamer discharge.
Finally the *Breakdown* module simulates the critical conditions which are produced by the electric breakdown across the interelectrodic gap, and the *Back corona* module takes into account the counteremission which is produced by micro-discharges in the high resistivity ash layers on the precipitator walls.

The third section includes the modules *Particle charging , Particle migration and current field* and *Space charge distribution*.
Particle charging considers the progressive charging of dust particles, starting from the inlet conditions up to saturation.
The module *Particle migration and current field* is used to compute the ion and particle motion; it takes into consideration all the forces applied to the particles, (i.e. viscous, electrical and gravitational), and the processes of charge exchange and turbolent diffusion. The motion of both ions and particles, which present different charge levels, concur to create the current field, which is calculated all over the interelectrodic space each time step.
Finally, the *Space charge distribution* module evaluates, each time step, the new charge distribution, which is necessary for updating the electric field distribution.

The fourth section is constituted by the modules *Particle collection, Rapping and reentrainment* and *Process efficiency*.
Once the charged particles distribution is known, the *Particle collection* module can simulate the laminar flow of both gas and particles near the collecting plate : this is considered as a sink where the collected particles disappear; the *Rapping and reentrainment* module simulates the injection of new particles that occurs inside the laminar flow region, either suddenly (rapping) or in a continuous manner (reentrainment due to flow erosion).
Finally, the *Process efficiency* module will determine the overall collection efficiency of the precipitator.

In order to describe in detail the physical processes listed above, a very fine three-dimensional grid discretization of the full precipitator would be needed.

However, such discretization is not feasible even if using large computers and therefore the precipitator is divided into elementary cells : each cell is large as a duct between two collecting plates, long as one or two plates and about 50 cm deep, as shown in the example of Figure 2.

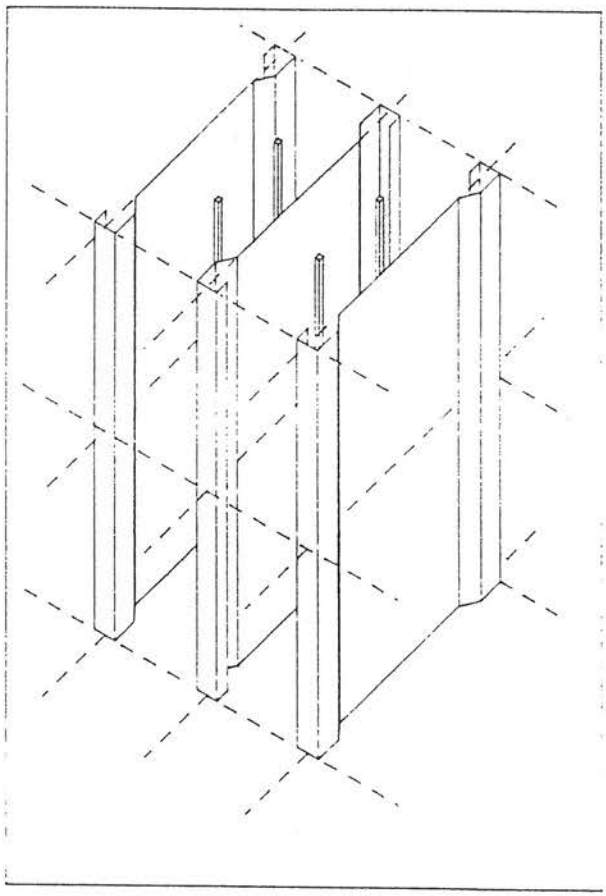

Fig. 2. Three dimensional view of a section of electrostatic precipitator showing the cell discretization.

Any simulation is thus performed in two steps : firstly, a three dimensional corse grid solution is determined in order to define the interface conditions among the cells. In particular it is assumed that the particle exchange between cells in the vertical direction is small with respect to the longitudinal direction, so that a bidimensional solution with the appropriate boundary conditions can be applied within each cell : in the second step the solution is recalculated on a finer mesh, in cascade for all the cells along the ESP ducts.

A solution scheme using a finite difference method is used with separate grids for each section or module; every grid is optimized with respect to local regions, with suitable finer meshes where the variable distributions present high gradients, or where is necessary to avoid numerical instabilities.
Appropriate interpolation and extrapolation routines are used to exchange data between different grides. The numerical algorithms of each module have been optimized in order to warrant a sufficient precision with a minimum computing time and memory usage. In the next paraghraph a detailed description of each module is given.

3. Gas and particles motion

The motion of particles in electrostatic precipitators is largely dominated by the motion of the gas in which the particles are suspended.
Regarding the gas as a continuum phase, its behaviour can be described by means of mass and momentum conservation laws, i.e. by the Navier-Stokes equations for turbulent flows.
Some useful simplifications are assumed :

- The fluid is not compressible because the mean flow velocity is lower then the sound velocity in the fluid.
- The flow is stationary on time scales longer then the turbolence characteristic time scale.
- The process is isothermal because the viscous and electric losses are negligible with respect to the initial gas entalpy.
- The gas flow is not influenced by the particle motion (no momentum is transferred from the dust particles to the fluid) because of their negligible relative concentration.
- Turbulence is assumed isotropic and described by a first order k - ε model.

Under these hypothesis the motion equations are[2] :

$$\frac{\delta v_k}{\delta x_k} = 0 \qquad (1)$$

$$\frac{\delta}{\delta x_k}(\rho v_k v_i) = -\frac{\delta p}{\delta x_i} + \rho g_i + \frac{\delta}{\delta x_k}\left[\mu\left(\frac{\delta v_i}{\delta x_k} + \frac{\delta v_k}{\delta x_i}\right)\right] \quad i=1,2,3 \qquad (2)$$

and the equations for the kinetic energy of turbulence k and the rate of turbulent dissipation ε are[3] :

$$\frac{\delta}{\delta x_i}(\rho v_i k) = \frac{\delta}{\delta x_i}\left(\frac{\mu_t}{\sigma_k}\frac{\delta k}{\delta x_i}\right) + \mu_t G - \rho\varepsilon \qquad (3)$$

$$\frac{\delta}{\delta x_i}(\rho v_i \varepsilon) = \frac{\delta}{\delta x_i}\left(\frac{\mu_t}{\sigma_\varepsilon} + \frac{\delta\varepsilon}{\delta x_i}\right) + \frac{\varepsilon}{k}(c_1\mu_t G - c_2\rho\varepsilon) \qquad (4)$$

where **v** is the local velocity of the fluid, ρ its density, p the pressure, **g** is the gravity acceleration, $\mu = \mu_{laminar} + \mu_t$ the effective coefficient of dynamic viscosity, with μ_t given by :

$$\mu_t = c_\mu \rho \frac{k^2}{\varepsilon} \qquad (5)$$

The source term G is defined as :

$$G = \frac{\delta v_i}{\delta x_k}\left(\frac{\delta v_i}{\delta x_k} + \frac{\delta v_k}{\delta x_i}\right) \qquad (6)$$

In order to calculate the particulate motion in the "Particle migration" module, the velocity field of the mean flow and the local coefficient of turbulent diffusion have to be computed within the precipitator volume.
The fluid-dynamic simulation is divided into two subsequent steps :

- In the first one a course grid three-dimensional solution based on the elementary cells discretization is obtained in order to describe the general characteristics of the gas flow and to define the flux transported across the walls of each elementary cell. At this stage of calculation the different wall profiles, the supports and the other structures are modelled by using local loss coefficients in the equations.

- In the second step each elementary cell is individually analyzed in detail, based on the boundary conditions defined by the coarse grid analysis. In this phase the vertical velocity component is assumed to be relatively small compared to the horizontal components; constant average values are therefore assumed on the upper and lower surfaces of the elemantary cell, and the fluid-dynamic simulation within the cell is reduced to a bi-dimensional analysis

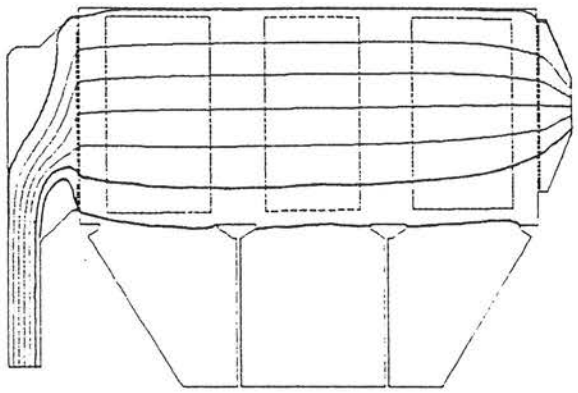

Fig. 3. Example of the gas flow lines in a longitudinal section of a model precipitator.

According to the electrode geometry an optimized non-uniform finite difference grid is generated over all elementary cells (see Figure 4); the equation system (1) to (6) is then solved to obtain the horizontal velocity components and the turbulence characteristic energy at all mesh points of any elementary cell.
An example of the coarse grid solution is given in Figure 3 for a longitudinal section of an idealized single hopper precipitator.
An example concerning with the solution of the detailed velocity field in two typical elementary cells with shaped walls is shown in Figure 4 . A uniform velocity profile of 1 m/s is imposed at the inlet and usual developed conditions at the outlet are assumed.
Small recirculations are shown close to the support structures along the walls; the core of the flow is similar to that developed for turbulent flows between parallel plate walls. As a preliminary sensitivity test, many different inlet conditions have been analyzed, in particular :

- Uniform velocity profiles close to 1 m/s.
- Velocity profiles corresponding to upstream developed flows.
- Uniform velocity profiles with transverse component.

The resulting detailed velocity field is quite similar for all the inlet conditions : this will probably make possible to simplify the analysis of subsequent cells in the same duct, by assuming that fully developed similar condition are reached after a small number of cells.

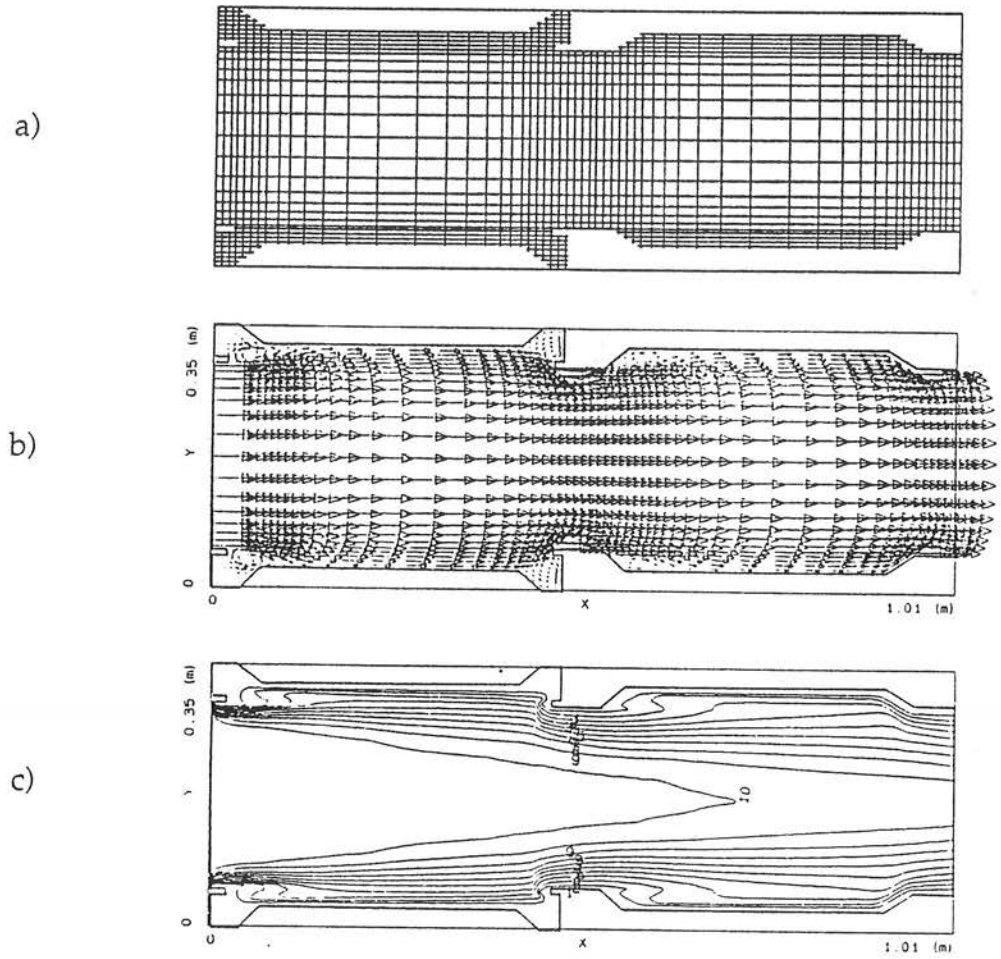

Fig. 4. Example of simulation on two elementary cells.
a) bidimensional finite difference grid
b) velocity field distribution
c) map of turbulent diffusion coefficient.

4. Electric field and Discharge processes

The particle collection in electrostatic precipitators is largely dominated by the distribution of the electric field in the interelectrodic space.
The electric field influences almost all the physical processes that occur in electrostatic precipitation. The field distribution defines the characteristics of the corona discharges, (either continuous glow or pulsed streamer) and therefore the ionic charge flux; the local electric field influences the particle charging and their saturation charge; the field magnitude defines the force that drags the particles towards the collecting plates; the field at the plane defines the electrostatic pressure that keeps compact the surface layer of fly ash and therefore influences the particulate reentrainment by hydrodynamic erosion and in correspondence of rapping.

4.1 Electric field

The module "Electric Field" calculates the distributions of the electric potential ϕ and of the corresponding electric field E by solving the Poisson equation :

$$\nabla^2\phi = \frac{\rho}{\varepsilon_0} \qquad (7)$$
$$E = -\nabla\phi$$

where ρ is the charge density and ε_0 is the dielectric constant.
The specific boundary conditions are given by the electrode geometry and applied voltages, and by the space charge distribution inside the precipitator volume.
In the time-dependent approach used in the present model the applied voltages and the space charge distribution may vary each integration time step, so that the electric field calculation has to be repeated at each time step, or in correspondence to any sudden variation of voltages (collapse due to breakdown) or space charge distribution (impulse corona occurence).
Under laplacian conditions, i.e. in absence of space charge, the electric field has essentially a planar symmetry, with identical values on parallel planes perpendicular to the vertical direction. Because of electrodes symmetry, the field distribution is identical in each elementary cell : it is therefore possible to limit the calculation to a single "sample" cell.
The presence of the space charge modifies the initial field conditions in the different elementary cells removing such symmetric properties: in fact the space charge distribution within the precipitator may change in the longitudinal direction because of the collection process, in the vertical direction because of the gravitational drag force and in the transversal direction because of non uniform and turbulent flow conditions. Each elementary cell has therefore to be treated individually : however, if the vertical component of the electric field is assumed negligible with respect to the horizontal one (it is in fact due only to vertical non-uniformities of the space-charge), the field calculation can be considered essentially a bidimensional problem.

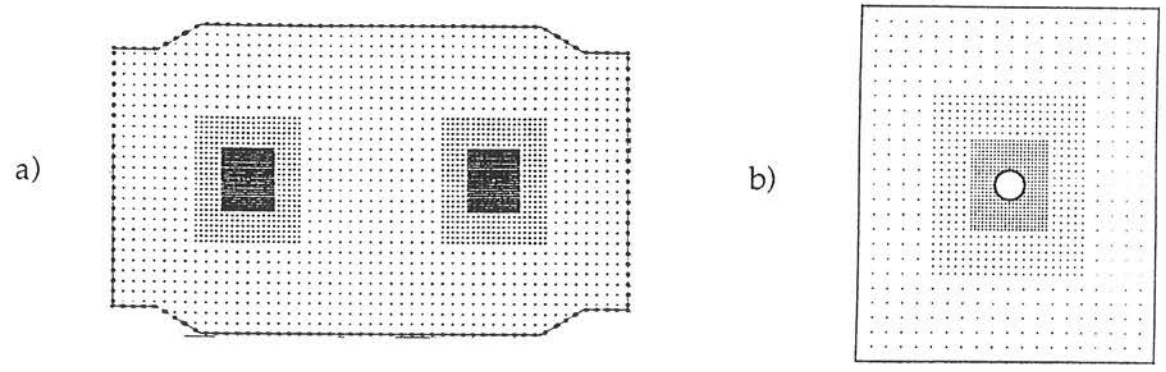

Fig. 5. Finite difference mesh used for electric field computation.
a) elementary cell; b) enlarged view on emitting wire

In all elementary cells a bidimensional non-uniform finite difference grid is applied : the mesh size decreases in the high field regions and is optimized on the basis of the laplacian field distribution (Figure 5); the geometric boundary grid points are automatically identified and the adequate voltage conditions are

assigned; the space charge value at each node, calculated from the *Space charge distribution* module on a different grid, is obtained by a fast bidimensional interpolation routine.

A fast iterative Poisson-Solver routine (assuming initial grid-point potentials derived either from the previous integration time solution or from the adiacent elementary cell) is then used to obtain the potential and field distribution in the cell, a typical example of which is reported in Figure 6.

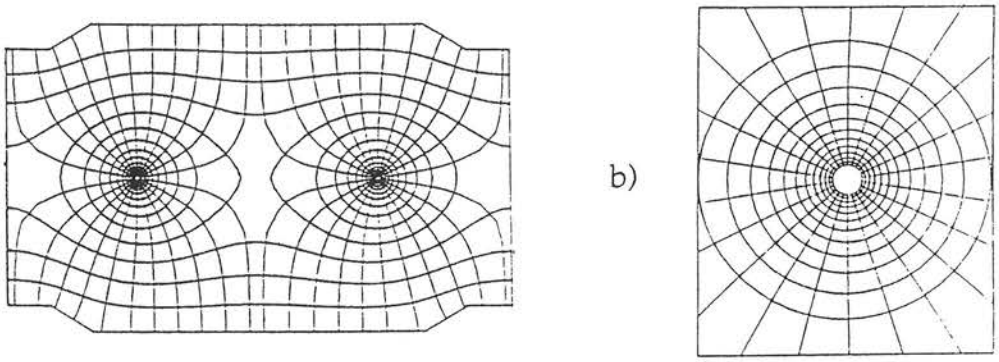

Fig. 6. Equipotential and field lines. a) elementary cell; b) enlarged view on emitting wire

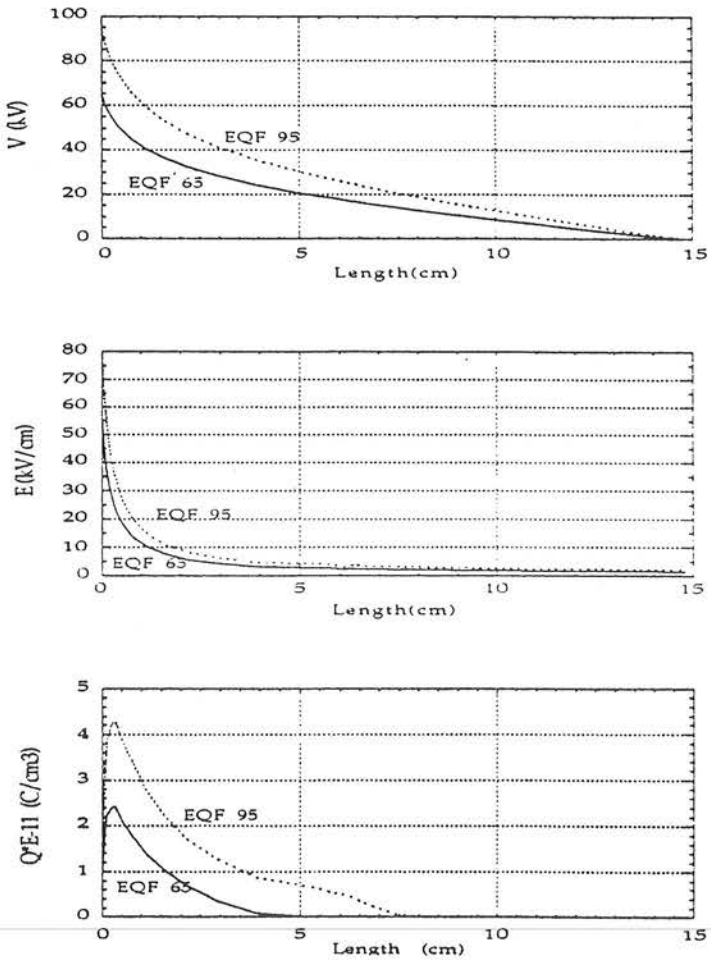

Fig. 7. Potential, field and charge density distributions along the maximum stress lines following an impulse corona discharge (at 65 and 95 kV).

4.2 Glow and streamer corona

In the configurations of electrostatic precipitators the ionic charge density changes in time because of the continuous or impulsive inlets due to discharges, and to the ion-particle attachment.
These phenomena are characterized fundamentally by the electric field distribution, so they can be treated as bidimensional processes and evaluated over the same grid as the electric field.
The glow corona discharge is confined in a small, bright region near the high voltage electrode (ionization region), where ionization processes can occur in the form of electron avalanches. The ions produced in the ionization region drift outside towards the plate electrodes (drift region).
The border of the ionization region is defined by the "critical field", for which ionization and attachment balance each other; the ionization can grow in an exponential way within an electron avalanche only when the field is higher than the critical value : in an electrostatic precipitator only a narrow sheath around the wire is used to produce electrons and ions, while in the outside region the ions are moved to reach the fly ash particles and to charge them.
In order to simulate the glow corona different approaches can be used[4,5]. The more reasonable one is to assume that the ionization region is a thin sheath, and that from the border of the ionization region a ionic current is injected into the drift region. The phenomena occuring inside the ionization region are taken into account only through a V-I characteristics : their overall effect is represented by the injection of an ionic current. If the ionization region is small enough, this current can be assumed to flow directly from the surface of the HV wire : it represents the ion flux boundary condition for the particle migration module.
The V-I characteristics are separately calculated by the joint integration of the current continuity and Poisson's equations in the interelectrodic space, with a technique described in the companion paper[6].
In ESP operation with continuous or slowly changing voltages, the glow corona is represented by a specific current boundary condition at the emitting wires, which varies in accordance to the instantaneous applied voltage.
In the case of impulse streamer corona the physical processes are very different from those of the DC glow corona : the streamer corona is not limited only to a small portion of the gap around the HV electrode, but is formed by a large number of branched filaments developing from the HV electrode into the high field region. At the tip of the filaments there is the high field region which represents a small ionization region, where electron avalanches are localized. This ionization region can move as a wave and produces the advancing mechanism of the streamer[7].
The main difference between glow corona and streamer corona is simply that in the former the field is produced only by the electrode geometry and thus the high field region is limited around the HV electrode; in the case of impulse corona the initial avalancing electrons build up a concentrated space charge, which distorts the field; the subsequent avalanches are able to reproduce this space charge into the gap, producing a local high field wave which can move into the space.
Different numerical models have been proposed to simulate the streamer propagation[8,9,10] : however they are computationally too heavy for massive use in the present ESP model.

Recently a simplified model based on an analytic solution of the propagation energy balance has been proposed[11]. It makes possible to simulate the propagation of a streamer filament along a field line and to calculate the net charge which is deposited along the propagation path, depending on the corresponding potential profile.
The actual program calculates the field line distribution from the emitting wires to the collecting planes (Figure 6), then it simulates the streamer propagation characteristics along each of them (Figure 7). At the end the filament charge is averaged over the finite difference grid in order to obtain the local value of the space charge ρ (Figure 8), which are in turn to be used for the subsequent field calculations.

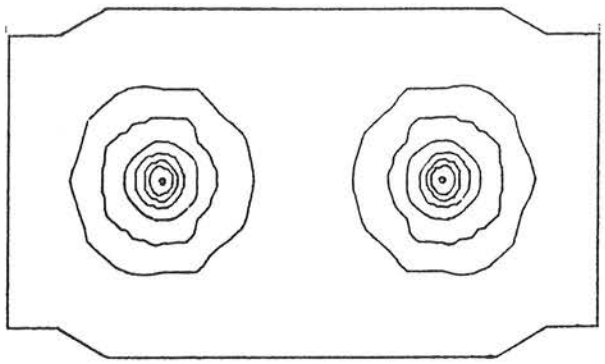

Fig. 8 Example of equicharge lines following an impulse corona discharge (95 kV applied voltage).

5. Particle charging and migration

The particulate path in the ESP depends upon its size and charge and thus the particles population may be classified on the basis of these two parameters. Its density distribution is then represented as a matrix whose rows (with index k) represent size classes and columns (with index j) charge classes. The assumed hypothesis that dust particles are the disperse phase in the continuum gas implies that there is no significant interaction between them, thus allowing to describe the behaviour of each class (k,j) of particles separately.
During the transport the particles can not change their size, i.e. can not move from one size class to another, while a progressive charging phenomenon takes place, forcing some particles belonging to charge class j to move to class j+1.
This charging is caused by ion and electron attachment to particles, due to both electric field and diffusion effects.
The first mechanism is dominant when the particle radius is greater than about 1.0 μm, while diffusion mechanism predominates on particles with a radius less than about 0.5 μm.
Particulate charging by field effect occurs because of the presence of particles cause a localized deformation of the electric field. The ions and electrons move under the influence of the applied electric field along the flux lines, and since these intercept the particulate, there is a collision between ions and particles with a consequent charging up of the latter.

The ionic charge continues to flow to the particle, and the process increases the charge of particulate until a sufficient electrostatic field is established in the vicinity of the particle by the retained charge to effectively repel the ions. This fact occurs when the field generated by charge q_s, called saturation charge, just balances the applied external field.
Diffusion charging results from collisions between ions and particles that occur because of the random thermal motion of the ions. This phenomenon can be described in terms of kinetic theory of gases.
It can be shown that the combination of these two mechanisms leads to the following expression for the charge rate of change with time[12] :

$$\frac{dq}{dt} = \frac{q_s}{t}\left(1-\frac{q_j}{q_s}\right)^2 + R_k^2\, e\, \rho_i \sqrt{\frac{8kT\pi}{m_k}}\, \exp\left(-\frac{q_j e}{R_k kT}\right) \qquad (8)$$

where q_j, R_k, m_k are respectively particle charge, radius and mass, ρ_i is ionic density, k is the Boltzmann constant, e the electron charge and T the gas temperature, and the the saturation charge q_s is defined as :

$$q_s = 12\,\frac{\kappa}{\kappa+2}\,\pi\,\varepsilon_o\, R_k\, E \qquad (9)$$

where κ is the relative dielectric constant and E the external electric field.

The particle migration process is solved by a lagrangian-eulerian mixed method. This approach allows to take into account both the deterministic component of the particulate motion, due to the newtonian forces, and the statistical behaviour related to random interactions, such as thermal motion and fluid turbulence.
Using a lagragian approach the path of every single particle is obtained by the integration of classic space and time equations, with fixed initial conditions and gravitational, electrical and viscous forces applied, such as :

$$m_k \frac{d\mathbf{v}_j^k}{dt} = m_k\mathbf{g} + q_j\mathbf{E} + 6\pi R_k \eta\,(\mathbf{v}_f - \mathbf{v}_j^k) \qquad (10)$$

where $\mathbf{v}_j^k$ is the velocity of a particle belonging to the k-th size class and j-th charge class, $\mathbf{g}$ is the gravity acceleration, η the dynamic viscous coefficient and $\mathbf{v}_f$ the gas velocity.

This differential equation can be easily solved under the hypothesis that electric field and gas velocity field do not vary in the time interval, Δt, necessary to cross the cell. Solution of eq. (10) is given by :

$$\mathbf{v}_j^k(\mathbf{r};t) = \mathbf{v}_f + \tau_j^k \frac{q_j}{m_k}\mathbf{E} + \tau_j^k\mathbf{g} + \left[\mathbf{v}^o - \left(\mathbf{v}_f + \tau_j^k \frac{q_j}{m_k}\mathbf{E} + \tau_j^k\mathbf{g}\right)\right] \exp\left\{-(t/\tau_j^k)\right\} \qquad (11)$$

where τ_j^k is relaxation time and $\mathbf{v}^o$ is the initial condition.

Provided that the value of the relaxation time τ_j^k is small with respect to the integration time Δt, than the velocity v (of the particle belonging to class (k,j)) can be assumed equal to its asymptotic value :

$$\mathbf{v}_j^k(\mathbf{r};t) = {}^{\alpha}\mathbf{v}_j^k(\mathbf{r};t) = \mathbf{v}_f + \tau_j^k \frac{q_j}{m_k}\mathbf{E} + \tau_j^k \mathbf{g} \qquad (12)$$

This equality means that particles reach a drift condition which is in equilibrium with the local applied forces. In such case it is possible to superimpose the velocities, instead of the forces, and therefore to consider an eulerian approach to describe the particulate motion.
Using this kind of modelization the behaviour of the particle population for every size and charge class (k,j) is described by Boltzmann's equation as[13]:

$$\frac{\delta \rho_j^k}{\delta t} + \mathrm{div}(\rho_j^k {}^{\alpha}\mathbf{v}_j^k - \nabla_r (D \rho_j^k)) = S_{j-1} - S_j \qquad (13)$$

where the lagrangian velocity term ${}^{\alpha}\mathbf{v}_j^k$ is representative of the entire class (k,j); D is the coefficient of turbolent diffusion and ρ_j^k is the particles density of the k-th size class and j-th charge class, while the source terms S_{j-1} and S_j account for the particle charging, that is S_{j-1} is the rate of particles of k-th size class moving from class j-1 to the higher class j, (and similarly for the term S_j).
The term S_j can be expressed as :

$$S_j = \frac{dq_j}{dt}\frac{1}{q_{j+1}}\rho_j^k \qquad (14)$$

6. Particle collection

The modules of this last section evaluate the quantity of dust particles collected at the plates. This evaluation considers several contributions :

- the istantaneous distribution of particulate;
- the various force fields that act on the particulate;
- the reentrainment characteristics of the particulate detaching from the plates and entering again into the gas flow.

6.1 Particle collection

The module simulates in detail the boundary layer near the collecting plates and the interchange that take place.
The following boundary conditions are assigned :

- towards the bulk of the gas flow : as defined on the surface of the last cell used in the Gas flow module
- towards plate surface : as computed by the "Rapping-Reentrainment" module which describes the reentering of particulate into the interelectrodic space.

At each time step the rate of dust particles attached on the collecting plates is evaluated for every size class k and charge class j.
In this way the characteristic of the deposited layer can be determined.

6.2 Rapping - Reentrainment

The particulate re-entering in the main stream presents two regimes : continuous and instantaneous.
The continuous detachment of particles from the plates is mainly due to dynamic erosion; the tangent velocity of the gas induces aerodynamic forces over the dust layer surface that are the viscous friction of the continuous phase (gas) and the bombardment of the dispersed phase (particles).
These continuous forces are able to win the electrical and chemical cohesion of the dust, therefore causing the detachment of a fraction of particles already collected on the plates.
This process is modelled with a flow of particles from all the plate surfaces towards the interelectrodic space, and needs the definition of some empirical parameters, similarly to erosion models such as the "cutting wear model".
The istantaneous detachment and reentrainment of particulate is so defined because of its very fast development compared with the integration time step, and it occurs only in some delimited areas of the entire collecting plate surfaces.
It is a random dust cloud typically caused by a discharge process (breakdown between wires and plates) and the phenomenon is simulated by a source point of particles.

The rapping process is a non-stationary phenomenon that causes also particulate reentering.
It is analyzed with a fractionary model. Part of the dust particles collected on the plates falls into the hoppers, part is retained onto the plates because of mechanical adhesion and electrostatic pression, and part enters again in the gas flow where is uniformly dispersed.

7. Conclusions

The present paper has described the general characteristics of a new mathematical model on electrostatic precipitators behaviour.
The model aims to overcome some of the limitations of existing semi-empirical models, base on the Deutsch equation and experimental data obtained from previous installations. Therefore the model will use an essentially physical approach with a time dependent development.
Starting with a 3-D discretization, it will be then solved as a bidimensional problem for redefined local approximations.
Each physical phenomenon of the precipitation process will be solved by a separate module with an exchange of information among different modules. It will be therefore possible, merely by upgrading the modules, to implement in the future any phenomena that will be considered to have been treated too roughly or any new phenomena that were to be considered of interest.

References

1. B. Bellagamba, E. Lami, F. Mattachini, A. Pigini, C. Valagussa, A. Martinelli. *"Laboratory tests for the study of fluid flow and corona characterization inside wire-plates structures of electrostatic precipitators"*, V ICESP, Washington DC, 1993.

2. R. B. Bird, W. E. Stewart, E. N. Lighfoot. *"Transport Phenomena"*, J. Wiley & Sons, 1960.

3. B. E. Launder, D. B. Spalding. *"Mathematical Models of Turbulence"*, Academic Press, N.Y., 1972.

4. R.S. Sigmond. *"Simple approximate treatment of unipolar space-charge-dominated coronas : the Warburg law and the saturation current"*, J. Appl. Phys., 53, pp. 891-898, 1982.

5. J.E. Jones, H. Davies. *"A critique of the Deutsch assumption"*, J. Phys. D. :Appl. Phys, 25, pp 1749-1759, 1992.

6. E. Lami, F. Mattachini, I. Gallimberti, R. Turri, U. Tromboni. *A numerical procedure for computing the voltage-current characteristics in ESP configurations"*, V ICESP, Washington DC, 1993.

7. I. Gallimberti. *"The mechanism of the long spark formation"*, J. de Physique C.7, 40, pp. 193-250, 1979.

8. I. Gallimberti. *"A computer model of streamer propagation"*, J. Phys. D: Appl. Phys., 5, pp. 2179-2189, 1972.

9. R. Morrow. *"Theory of negative corona in oxygen"*, Phys. Rew. A 32, pp. 1799-1809, 1985.

10. C. Wu, E. E. Kunhardt. *"Formation and propagation of streamers in N_2 and N_2-SF_6 mixtures"*, Phys. Rew.,A 37, pp. 4399-4406, 1988.

11. S. Badaloni, I. Gallimberti, E. Marode. *"A simplified model of streamer formation in weakly electronegative gases"*, in course of pubblication on J. Phys. D: Appl. Phys.

12. S. Oglesby Jr., G. B. Nichols. *"Electrostatic Precipitation"*, Marcel Dekker Inc. N.Y., 1978.

13. A. Gilardini. *"Low energy electron collisions in gases"*, John Wiley & Sons, N.Y., 1972.